



ChemComm

Carrier Protein Mediated Cargo Sensing in Quorum Signal Syntheses

Journal:	<i>ChemComm</i>
Manuscript ID	CC-COM-06-2022-003551.R1
Article Type:	Communication

SCHOLARONE™
Manuscripts

COMMUNICATION

Carrier Protein Mediated Cargo Sensing in Quorum Signal Synthases

Patrick D. Fischer^{a,c,d}, Abu Sayeed Chowdhury^f, Thomas Bartholow^e, Shibani Basu^b, Eric Baggs^b, Huel S. Cox III^{a,c}, Srđan Matošin^{a,c}, Michael D. Burkart^e, Lisa Warner^b, Rajesh Nagarajan^{b*} and Haribabu Arthanari^{a,c*}

Received 00th
January 20xx,
Accepted 00th
January 20xx

DOI:10.1039/x

Acyl-homoserine lactone synthases make specific AHL quorum sensing signals to aid virulence in Gram-negative bacteria. Here, we use solution NMR spectroscopy to demonstrate the carrier protein-enzyme interface accurately reveals substrate recognition mechanisms in two quorum signal synthases.

Gram-negative bacteria count specific *N*-acyl-L-homoserine lactone (AHL) quorum sensing autoinducer signals to estimate population density. Quorum sensing (QS) enables bacteria to activate virulence traits such as biofilm formation, sporulation, toxin production, antibiotic resistance in a cell-density-dependent manner.¹ To ensure efficient cell-counting of their species, signal-synthesizing enzymes such as AHL synthases precisely make the native signal for that bacterium and avoid synthesizing nonspecific signals (**signal fidelity**). The acyl-homoserine lactone signal has two important moieties: the conserved lactone head group and the variable acyl chain (derived from the acyl chain of the acyl-ACP substrate, Figure 1). AHL synthases have therefore evolved to selectively recognize a specific acyl-ACP substrate to enforce fidelity in signal synthesis. The molecular details on how protein-protein communication promotes specificity in signal synthesis remain unresolved.

Acyl carrier proteins serve as indispensable cofactors in both primary and secondary metabolic pathways delivering sequestered chemical cargoes from the ACP core to the active sites of dozens of enzymes and regulatory proteins.² The pathway for acyl-ACP binding to an AHL synthase involves two steps: an initial electrostatic mediated docking of acidic residues (mostly from helix II of the carrier protein) on to a basic patch in the partner enzyme followed by enzyme-assisted cargo flipping from the ACP to the enzyme acyl-chain pocket. Once the cargo settles in the enzyme's acyl chain pocket, the phosphopantetheine and the carrier protein moieties of the acyl-ACP substrate are then stationed in place to form a catalytically competent [E.acyl-ACP.SAM] ternary complex. A

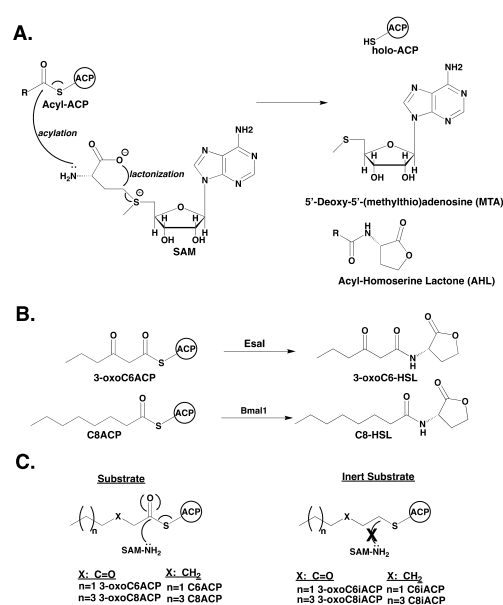


Figure 1. Substrates and products of AHL synthesis. A. Mechanism of AHL synthesis. B. Acyl-substrate and AHL products of Esal and Bmal1-catalyzed AHL synthesis. C. Alkyl-ACP inert substrates used in this study.

productive ternary complex would then optimally position the two substrates for the acylation and lactonization chemical steps to complete AHL synthesis.³ Ternary complexes with non-native substrates, in principle, could either be *less productive* (substrate binding in a non-optimal mode leading to slower chemistry and/or product release steps) or *unproductive* promoting cargo flipping back to ACP and substrate dissociation. Overall, the degree of catalytic competence of enzyme-substrate complexes is expected to follow similar trends as their corresponding substrate catalytic efficiencies. In this study, we used a combination of NMR, kinetics, and docking methods to reveal structural insights into the differences between productive and unproductive enzyme-substrate complexes. Here we investigate a substituted-cargo-preferring *Pantoea stewartii* Esal and an unsubstituted-cargo-preferring *Burkholderia mallei* Bmal1 AHL synthase. *Pantoea stewartii* is a plant pathogen that causes Stewart's wilt and leaf blight disease in rice, maize etc.⁴ This bacterium uses Esal AHL synthase to create 3-oxohexanoyl homoserine lactone (3-oxoC6-HSL)

^a Department of Biological Chemistry and Molecular Pharmacology, Harvard Medical School, Boston, MA, USA.

^b Department of Chemistry and Biochemistry, Boise State University, Boise, ID, USA.

^c Department of Cancer Biology, Dana-Farber Cancer Institute, Boston, MA, USA.

^d Department of Pharmacy, Pharmaceutical and Medicinal Chemistry, Saarland University, Saarbrücken, Germany.

^e Department of Chemistry and Biochemistry, University of California, San Diego, CA, USA.

^f Biomolecular Sciences Graduate Program, Boise State University, Boise, ID, USA

autoinducer signals to enable the cell-density dependent production of exopolysaccharide (EPS) and increased virulence.⁴ Esal selectively recognizes 3-oxohexanoyl-ACP as the acyl-donor substrate to produce 3-oxohexanoyl-homoserine lactone (3-oxoC6-HSL, Figure 1). Two AHL synthase isoforms Bmal1 and Bmal3 in *Burkholderia mallei*, preferentially recognize C8-ACP and 3-hydroxyC8-ACP substrates, respectively, to make the octanoyl homoserine lactone (C8-HSL) and 3-hydroxyoctanoyl homoserine lactone (3-hydroxyC8-HSL) QS signals.⁵ To capture enzyme-substrate complexes, the reactive thioester in acyl-ACPs were replaced by a thioether to form the corresponding "alkyl-ACPs" (Figures 1C and S1). Cargo loading was accomplished through *in vitro* phosphopantetheinylation of ¹³C/¹⁵N- or ¹⁵N-labelled *E. coli* apo-ACP with the alkyl-CoA substrates shown in Schemes S1 using the recombinant 4'-phosphopantetheinyl transferase Sfp from *Bacillus subtilis*.^{3a} Correct loading was confirmed by intact mass spectrometry analysis (Figures S20-S23). A suite of triple resonance backbone experiments was then recorded on ¹³C/¹⁵N-labelled carrier proteins to unambiguously assign backbone resonances for apo ACP, octyl-ACP (C8iACP) and 3-oxohexyl-ACP (3-oxoC6iACP) (Figures S4, S5 and S10).

Chemical Shift Perturbation (CSP) analysis is a common method to identify binding sites in protein-ligand complexes using NMR. The chemical shift of an NMR-active nucleus is sensitive to its local electronic environment. Ligand binding to a protein will produce CSPs at the ligand binding site and at allosteric sites that undergo conformational changes due to the binding event.⁶ Here, we observed CSPs between apo-ACP vs. 3-oxohexyl-ACP and apo-ACP vs. octyl-ACP pairs. In both cases, significant CSPs are observed on helices II-IV. The interior side of these three helices provide the pocket for sequestering part of the phosphopantetheine and the alkyl-chain cargo moieties of the alkyl-ACP. The CSPs observed were plotted as a heatmap onto the structure of heptanoyl ACP (PDB ID 2FAD, Figure S10)⁷.

The kinetic constants for the native and non-native substrates for Esal and Bmal1 investigated in this study are summarized in Table S1. To identify the residues on ACP that interact with their respective AHL synthases, ¹⁵N-labelled loaded alkyl-ACPs were titrated with increasing concentrations of unlabelled AHL synthases. For final analysis, all CSPs were calculated from a ratio of 1 equivalent ACP to 1.5 equivalents AHL synthase. Interestingly, irrespective of the order of addition (alkyl-ACP + SAM mixture titrated with enzyme or alkyl-ACP titrated with enzyme preincubated with SAM), we observed that the ACP CSPs were identical and the addition of SAM did not result in additional CSPs. This result suggests that the enzymes conformational change upon SAM addition, if any, must be localized at its substrate binding site, keeping the carrier protein contacting face of the enzyme unaffected. For the chosen experimental conditions, both [Esal.3-oxoC6iACP] and [Bmal1.C8iACP] interactions took place in an intermediate exchange regime, leading to peak broadening rather than population-weighted chemical shift changes. The CSPs (in case of apoACP.Esal) or intensity reductions (in case of apoACP.Bmal1) are significantly lower when compared to those observed with the native cargoes (Figures S17 and S18). The [Enzyme.Native cargo-loaded ACP] complexes (such as the [Esal.3-oxoC6iACP] and [Bmal1.C8iACP]), however, displayed significantly more CSPs when compared to the [Enzyme.apo-ACP] complex, ([Esal.apo-ACP] or [Bmal1.apo-ACP]). This indicates that presence of the cargo is conducive for the ACP's interaction with the enzyme. In the case of [Esal.3-oxoC6iACP] ES complex, strong CSPs were observed on the acidic residues of the ACP, including D35, D38, E41, E47 and E48 highlighting the

importance of electrostatics in the ACP-enzyme interaction (Figures 2, S8, S11 and S19). The majority of CSPs are localized to the ACP helix II in case of the [Esal.3-oxoC6iACP] interaction. The CSPs were widespread for the [Bmal1.C8iACP] interaction, starting at the C-terminal portion of helix II and extending to loops 2 and 3 and helices

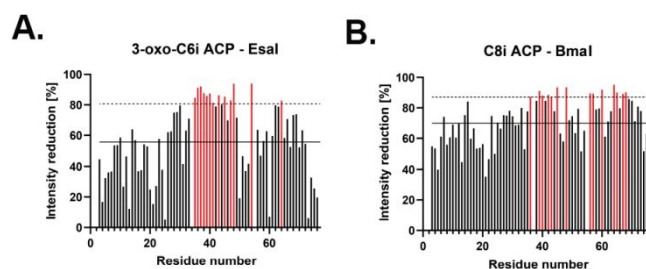


Figure 2. Intensity reduction analysis of productive ES complexes. A. 3-oxohexyl-ACP with and without Esal. B. Octyl-ACP with and without Bmal1.

III and IV. Helix II of the ACP contributes to hydrophobic interactions while electrostatic interactions are more confined to loop 2 and helix III in the C8iACP-Bmal1 pair (Figures 2, S9, S12 and S19). While the overall amino acid sequence identity of *E. coli* ACP relative to *B. mallei* and *P. stewartii* ACPs are 74% and 90% respectively, the identities among the residues in helices II, III and loops 2 and 3 (the regions experiencing CSPs) among the three ACPs is > 95% (Figure S3). We then investigated if the broad range of CSPs observed in the [Bmal1.C8iACP] complex could arise from an artifact due to using the *E. coli* ACP_e in lieu of *B. mallei* ACP_b. To address this question, we replaced the *E. coli* ACP_e with the cognate ACP_b from *B. mallei* in the C8iACP and titrated it with the Bmal1 enzyme. The intensity reductions for [Bmal1.C8iACP_b] were similar to the [Bmal1.C8iACP_e] highlighting the fact that CSP differences observed between [Esal.ACP] and [Bmal1.ACP] complexes are valid and independent of differences in amino acid identities among the two carrier proteins (Figure S13). The above data suggests that i) Esal and Bmal1 use distinct interfaces to engage with their corresponding native acyl-ACPs and ii) the specificity of ACP-enzyme interactions is enhanced only in the cargo-loaded carrier protein. To delineate the structural differences between *productive vs. less-productive vs. unproductive* enzyme-substrate complexes in Esal-catalyzed AHL synthesis we made the following non-native alkyl-ACPs: the 3-oxoC8iACP (increase in chain length relative to 3-oxoC6iACP, assignment shown in Figure S6) and C6iACP (devoid of the 3-oxo moiety, assignment shown in Figure S7). The catalytic efficiencies of the corresponding substrates followed the order: Furanacetyl-ACP (3-oxoC6-ACP mimic, forms *productive* ES complex; k_{cat}/K_m of $0.37 \pm 0.05 \mu\text{M}^{-1}\text{s}^{-1}$) > Benzofuranacetyl-ACP (3-oxoC8-ACP mimic, forms *less productive* ES complex; k_{cat}/K_m of $0.05 \pm 0.006 \mu\text{M}^{-1}\text{s}^{-1}$) > C6-ACP (forms *unproductive* ES complex, k_{cat}/K_m of $0.008 \pm 0.001 \mu\text{M}^{-1}\text{s}^{-1}$; Table S1, Figure S14A).⁸ We were able to assign residues in the HSQC spectra of these new alkyl-ACPs without the need for additional triple resonance backbone experiments, due to the proximity of peaks with respect to 3-oxoC6iACP and C8iACP (Figures S6 and S7). The ¹⁵N-labelled alkyl-ACP samples were then titrated with Esal and HSQC spectra were acquired to determine which ACP residues underwent chemical shift perturbations. The NMR data shows that [Esal.3-oxoC8i ACP] binding interface closely resembles the [Esal.3-oxoC6iACP] interface, consistent with the similar K_m and catalytic efficiencies between these two substrates with the Esal enzyme. In addition, the average reduction in peak intensity of ~62% in the [Esal.3-oxoC8i ACP] is similar to the ~56% reduction observed in the [Esal.3-oxoC6i ACP].

The binding of C6iACP with Esal, however, was in a fast exchange regime, leading to the observance of CSPs rather than intensity reduction, characteristic of the intermediate exchange regime. We note that a majority of helix II CSPs that had shifted in the [Esal.3-oxoC8iACP] complex was not observed in the [Esal.C6iACP] complex (Figure S11). To further investigate the role of the 3-oxo moiety in substrate recognition for the Esal, the T140 residue in the acyl-chain pocket was mutated to alanine (the T140 residue is within hydrogen bonding distance to the oxygen atom in the 3-oxo group).⁹ The C6-ACP, while a poor substrate for the wild-type enzyme is an excellent substrate for the T140A mutant version of the Esal (Table S1).⁸ Like the [Esal.3-oxoC6iACP] and the [Esal.3-oxoC8iACP] complexes, the [EsalT140A.C6iACP] complex retained most CSPs in the helix II with ~74% average intensity reduction (Figure S11). These results suggest that modifying the 3-oxo functionality is more deleterious than changing the cargo chain lengths in the Esal-catalyzed AHL synthesis.

Bmal1 was titrated to the following ¹⁵N-labelled, non-native cargo-loaded ACP samples: C6iACP (decrease in chain length from C8) and 3-oxoC8iACP (introduction of the 3-oxo moiety to the C8 chain). The catalytic efficiencies of the corresponding substrates follow the order: C8-ACP > Benzofuranacetyl-ACP (3-oxoC8-ACP mimic) ~ C6-ACP (Table S1, Figure S14A).^{3a} All interactions of ACPs with Bmal1 took place in an intermediate exchange regime, hence we compared the reduction in peak intensity in these cases. While the average intensity reduction for the [Bmal1.C8iACP] complex was ~70%, it reduced to ~25% for the [Bmal1.apo-ACP] interaction, ~32% for the [Bmal1.C6iACP] interaction and ~44% for the [Bmal1.3-oxoC8iACP] complexes (Figures 2 and S12). In addition, the interaction with the secondary binding site on helix III between residues ~56-60 was not pronounced for either of the non-native cargoes. Unlike Esal, both 3-oxoC8iACP and C6iACP non-native cargoes had a similar effect on the binding interface between ACPs and Bmal1. In summary, the major findings of this study are: i) both Esal and Bmal1 only minimally interact with apo-ACP while forming distinct, signature interfaces with their corresponding native cargo-loaded ACPs ii) the CSPs for the [Esal.3-oxoC6iACP] complex are mostly localized to ACP helix II but more widespread for the [Bmal1.C8iACP] encompassing the helices II-IV and loops II & III revealing differences between the two productive ES complexes iii) Esal and Bmal1 adopt different mechanisms to recognize non-native substrates (discussed below) iv) the ACP-enzyme interface reflects the innate cargo preferences (substituted vs. unsubstituted) for the partner enzyme.

Cargo Recognition by Esal. In the [Esal.3-oxoC6iACP] complex, the Thr140 residue forms a hydrogen bond to the substrate C3 oxygen atom, effectively locking the 3-oxoC6 cargo-chain in the enzyme acyl-chain pocket (Figure S2).^{8,9} With the cargo chain tightly locked in the enzyme acyl-chain pocket, less of the ACP surface is then required to form the carrier protein-enzyme binding interface. The enzyme therefore makes minimal, but strong and specific contacts, confined to the helix II of the ACP. Since the catalytic efficiency of the 3-oxoC8-ACP with Esal is ~7-fold less (K_m increases by a factor of 2, Table S1) compared to the 3-oxoC6-ACP, this substrate should form a *less productive* enzyme-substrate complex relative to the native substrate. Although the 3-oxo moiety in the 3-oxoC8iACP is capable of hydrogen bonding to Thr140 residue, the increased chain length forces the cargo to bind in a less optimal conformation. A weakly bound cargo is reflected in the loss of CSPs in the carrier protein helix II (E41, V43, A45 and E48) which are compensated by additional, nonspecific CSPs in loop 1 (E20, E30, D31), loop 3 (T63) and helix IV

(Q66 and I69). The C6-ACP is the poorest among the two non-native Esal substrates with its k_{cat}/K_m about 40-fold lower than 3-oxoC6-ACP and 6-fold lower than 3-oxoC8-ACP (Figure S14A). In line with the kinetics observations, this substrate has the fewest CSPs among the Esal substrates investigated in this study (Figures 2 and S11). The CSPs for the *unproductive* [Esal.C6iACP] complex are spread out among loops 1-3 and helices II-IV. Most importantly, the 3-oxoC6 chain-specific CSPs formed between helix II and Esal are almost entirely lost in this ES complex (Figure S19). These observations highlight the differences between *productive* ([Esal.3-oxoC6iACP], localized to helix II), *less productive* ([Esal.3-oxoC8iACP], minor loss in helix II CSPs with gain in additional nonspecific CSPs in other secondary structural elements) and *least productive* ([Esal.C6iACP], major loss of helix II-enzyme CSPs with a handful of nonspecific CSPs in other loops and helices) enzyme-substrate complexes. The extent to which Esal engages ACP helix II reflects the cargo type (substituted vs. unsubstituted, cognate vs. noncognate, etc.) bound at the enzyme's acyl-chain pocket.

Since CSPs report on a change in electronic environment, the CSPs observed on helix II could be because of the cargo flipping into the enzyme and/or a direct interaction with the enzyme. To establish a direct interaction between the ACP and the Esal, we performed cross-saturation transfer experiments (CST) with perdeuterated ¹⁵N labeled ACP. In CST experiments magnetization is transferred via saturation from a sample with signals in the aliphatic region (Esal in this case) to a sample with no signals in the aliphatic region (ACP). This transfer manifests as a reduction in intensity in the HSQC, at the site of contact, compared to control off-resonance part of the spectrum with no signals is saturated. CST experiments clearly show that the helix II of ACP is in direct contact with Esal (Figure S16)

Cargo Recognition by Bmal1. Bmal1 prefers an unsubstituted octanoyl-chain cargo. The nonpolar C8-chain of the C8-ACP substrate, however, cannot be effectively locked in the greasy acyl-chain pocket of Bmal1. In the absence of a locking mechanism, the cargo would have more degrees of freedom in the acyl-chain pocket and hence the extended protein-protein contacts might be necessary to keep the substrate bound to the enzyme. Accordingly, in the [Bmal1.C8iACP] complex, the distribution of ACP CSPs is far more spread compared to [Esal.3-oxoC6iACP] spanning helices II-IV and loops 2 and 3 (Figures 2 and S12). CSPs from helix II in the ACP predominantly arise from nonpolar amino acids while the electrostatic contribution dominates the CSP from helix III. Among the 3-oxoC8iACP and C6iACP non-native ligands, the CSPs of the former ligand closely resemble the native C8iACP ligand. Interestingly, a Thr145 residue (in the β_5 sheet) is positioned at the tip of the acyl-chain pocket (versus mid-pocket in Esal) that could potentially form hydrogen-bond with the 3-oxo moiety of the 3-oxoC8iACP ligand (Figure S2). The nonoptimal position of this hydrogen bond would render the lock less effective ensuing the formation of a *less productive* ES complex compared to the native C8iACP. If the 3-oxoC8 cargo-chain in Bmal1 is locked like the 3-oxoC6 chain in Esal, we should expect Bmal1 to engage more with ACP helix II. Indeed, the [Bmal1.3-oxoC8iACP] complex picks up additional polar interactions in helix II (reminiscent of [Esal.3-oxoC6iACP]) while retaining the electrostatic CSPs in helix III (as observed in [Bmal1.C8iACP]). The CSPs in [Bmal1.C6iACP] complex, however, are more localized to helix II and loop 2 (Figure S12). It is apparent that the carrier protein mediates cargo recognition via orthogonal mechanisms among the two enzymes investigated in this study. In the Esal enzyme, native cargo-loaded ACP CSPs are localized to helix II while their non-native counterparts display delocalized CSPs. The

scenario is opposite for Bmal1 where native cargo-loaded ACP CSPs are widespread while non-native cargo-loaded ACP CSPs are confined. In addition, the electrostatic contributions to the [Enzyme-ACP] complex arise from helix II in Esal and helix III in Bmal1 complexes (Bmal1 engages helix II via Van der Waals interactions). Whether this observation is specific for the Esal and Bmal1 enzymes or a general feature of substrate recognition in AHL synthases remains to be investigated.

The experimental data was used to dock the native and non-native ACPs on to Esal and Bmal1 to further comprehend the structural differences between the productive, less productive, and nonproductive ES complexes. The productive ES complex in Esal appears to include enzyme helices III, V and loop 8 while the Bmal1 counterpart has a larger enzyme surface footprint including helices I, II, V, loop2 and $\beta 8$ beta sheets (Figures S2, S14B and S15). The nonproductive C6iACP substrate bound orthogonally to the Esal face losing almost all specific interactions between ACP helix II and the enzyme observed in the productive ES complex. The binding mode of the less productive [Esal.3-oxoC8iACP] was intermediary between the productive and nonproductive modes. In agreement with the kinetics results, the binding poses of [Bmal1.3-oxoC8iACP] and [Bmal1.C6iACP] were similar revealing the nature of the less productive ES complex in Bmal1 catalysis.



Figure 3: Schematic depiction of cargo recognition mechanisms. The ACP/AHL-synthase interface is highlighted in orange and the cargo/AHL-synthase interface in pink. The Esal/3-oxo-C6i ACP complex displays a smaller ACP/Esal interface, while making use of a hydrogen bond between the 3-oxo moiety of the cargo and T140 of Esal. The Bmal1/C8i ACP complex on the other hand is has a larger ACP/Bmal1 interface.

The NMR studies reveal the innate cargo preference for the partner enzyme where the protein-protein interface is minimal for enzymes preferring substituted cargoes (such as Esal) and extended for enzymes preferring unsubstituted cargoes (Bmal1) (Figure 3). As a final test to this hypothesis, we mutated the Thr140 residue in Esal to alanine and determined the CSPs of [EsalT140A.C6iACP] complex. The C6-ACP is an excellent substrate for the Esal T140A mutant with a k_{cat}/K_m of $0.51 \pm 0.06 \mu\text{M}^{-1}\text{s}^{-1}$, comparable to the k_{cat}/K_m of $0.37 \pm 0.05 \mu\text{M}^{-1}\text{s}^{-1}$ for the 3-oxoC6-ACP substrate mimic reacting with the wild type Esal (Table S1).⁸ Based on the catalytic efficiencies, C6-ACP should behave like a native substrate for the Esal T140A mutant and thus the CSPs would be expected to match closely with the CSPs observed in [Esal.3-oxoC6iACP] complex. Since the acyl-chain cargo in C6iACP does not possess the 3-oxo substitution, we wondered if the carrier protein interface for the [EsalT140A.C6iACP] complex would be able to reveal the unsubstituted cargo preference for the mutant enzyme? Indeed, the CSPs observed for the [EsalT140A.C6iACP] complex is a hybrid of signature CSPs from both [Esal.3-oxoC6iACP] and [Bmal1.C8iACP] complexes, adding credence to the theory that carrier protein interfaces can reflect the nature of the cargo bound at the active site of the partner enzyme.

In summary, we note that the specific protein-protein interface of the 3-oxohexanoyl-ACP bound Esal is advantageous to enforcing specificity in cargo recognition over an extended interface observed in the octanoyl-ACP bound Bmal1 enzyme. A non-native

substrate binding to Esal could either lock the cargo-chain (the hydrogen bonding lock would be inefficient for shorter or longer chains) or maintain specific interactions with the helix II, but not both. Bmal1, on the other hand, could neither lock the cargo-chain nor confine the protein-protein interface. In fact, kinetic studies with native and non-native substrates reveal that Esal displayed tighter specificity to its native substrate compared to the Bmal1 (the Bmal1 enzyme makes both octanoyl-homoserine lactone and hexanoyl-homoserine lactone AHL signals in *B. mallei* QS). Unsubstituted cargo preferring AHL synthases would be less capable of rejecting nonspecific substrates at the binding step and thus would have to rely on slower acylation/lactonization or product release steps to enforce fidelity in quorum sensing signal synthesis.

Financial support for this project came from NSF-1905311 (RN, LW), NIH INBRE grants P20 RR016454 and P20 GM103408. PDF acknowledges the Chleck Foundation for financial support. HA acknowledges support from NIH (R01 GM136859). We thank Drs Philip Cole and Hwan Bae for assistance with mass spectrometry.

Conflicts of interest

There are no conflicts of interests to declare.

Notes and references

- 1 a) R. S. Smith, B. H. Iglewski, *Curr. Opin. Microbiol.*, 2003, **6**, 56; b) B. A. Duerkop, J. Varga, J. R. Chandler, S. B. Peterson, J. P. Herman, M. E. A. Churchill, M. R. Parsek, W. C. Nierman, E. P. Greenberg, *J. Bacteriol.*, 2009, **191**, 3909; c) B. K. Hammer, B. L. Bassler, *Mol. Microbiol.*, 2003, **50**, 101.
- 2 a) V. Agarwal, S. Lin, T. Lukk, S. K. Nair, J. E. Cronan Jr, *Proc. Natl. Acad. Sci. USA*, 2012, **109**, 17406; b) Y. J. Lu et al., *Mol. Cell*, 2006, **23**, 765; c) J. T. Mindrebo, L. E. Misson, A. Patel, W. E. Kim, T. D. Davis, Q. Z. Ni, J. J. La Clair, M. D. Burkart, *Comprehensive Natural Products III: Chemistry and Biology*, 2020, **1**, 61.
- 3 a) A. N. Montebello, R. M. Brecht, R. D. Turner, M. Ghali, X. Pu, R. Nagarajan, *Biochemistry*, 2014, **53**, 6231; b) A. Raychaudhuri, A. Jerga, P. A. Tipton, *Biochemistry*, 2005, **44**, 2974.
- 4 a) M.D. Koutsoudis, D. Tsaltas, T.D. Minogue, S. B. con Bodman, *Proc. Natl. Acad. Si. USA*, 2006, **103**, 5983; b) C. Aurelien, B. Lindsey, S. B. von Bodman, *Mol. Microbiol.*, 2009, **74**, 903.
- 5 a) B. A. Duerkop, J. P. Herman, R. L. Ulrich, M. E. A. Churchill, E. P. Greenberg, *J. Bacteriol.*, 2008, **190**, 5137; b) B. A. Duerkop, R. L. Ulrich, E. P. Greenberg, *J. Bacteriol.*, 2007, **189**, 5034; c) C. Majerczyk, L. Kinman, T. Han, R. Bunt, E. P. Greenberg, *Infect. Immun.*, 2013, **81**, 1471.
- 6 a) J. A. Purslow, B. Khatiwada, M. J. Bayro, V. Venditti, *Frontiers in Molecular Biosciences*, 2020, **7**:9; b) M. P. Williamson, *Progress in Nuclear Magnetic Resonance Spectroscopy*, 2013, **73**, 1.
- 7) A. Roujeinikova, W. J. Simon, J. Gilroy, D. W. Rice, J. B. Rafferty, A. R. Slabas, *J. Mol. Biol.*, 2007, **365**, 135.
- 8) M. N. Lam, D. Dudekula, B. Durham, N. Collingwood, E. C. Brown, R. Nagarajan, *Chem. Commun.*, 2018, **54**, 8838.
- 9) T. A. Gould, J. Herman, J. Krank, R. C. Murphy, M. E. A. Churchill, *J. Bacteriol.*, 2006, **188**, 77